Electronic Supplementary Information for:

Compositionally-Tunable Mechanochemical Synthesis of $Zn_xCo_{3-x}O_4$ Nanoparticles for Mesoporous P-type Photocathodes.

Shannon M. McCullough[†], Cory J. Flynn[†], Candy C. Mercado[‡], Arthur J. Nozik[‡,§], and James F. Cahoon[,†]*

[†]Department of Chemistry, University of North Carolina at Chapel Hill, Chapel Hill, NC 27599-3290. [‡]Renewable and Sustainable Energy Institute, and Department of Chemistry and Biochemistry, University of Colorado, Boulder, CO 80309-0027. [§]National Renewable Energy Laboratory, 15013 Denver West Parkway, Golden, CO 80401.

* Corresponding author. Email: jfcahoon@unc.edu

Supplementary information includes:

1. Experimental Methods
2. Supplemental Figures S1-S8
3. Supplemental Table S1

1. Experimental Methods.

1.1 Materials and Reagents.

Acetonitrile (99.6%), cobalt nitrate hexahydrate (reagent grade), iodine (>99.99%), lithium iodide, lithium perchlorate (>99%), and zinc nitrate hexahydrate (reagent grade) were all purchased from Sigma-Aldrich. Methyl methacrylate (MMA) and poly(methyl methacrylate) (PMMA) were purchased from Microchem. Absolute ethanol (Decon Laboratories), isopropyl alcohol (IPA; electronics grade), and sodium hydroxide (pellets/certified ACS) were purchased from Fisher Scientific. 25 μm thick Surlyn polymer was purchased from Solaronix. P1 chromophore was purchased from Dynamo. All chemicals were used as received. Fluorine-doped tin oxide (FTO) glass (TEC 15 $\Omega \cdot cm^2$) was purchased from Hartford glass and cleaned with typical organic solvents and sonication.

1.2 $Zn_xCo_{3-x}O_4$ Nanoparticle Synthesis

$Zn_xCo_{3-x}O_4$ was prepared by manually grinding together desired ratios of $Zn(NO_3)_2 \cdot 6H_2O$, $Co(NO_3)_2 \cdot 6H_2O$, and NaOH in an agate mortar and pestle for 3 minutes to form a hydroxide precursor, $Zn_xCo_{3-x}(OH)_6$. $Zn_xCo_{3-x}(OH)_6$ was rinsed with 50 mL deionized H_2O, collected via centrifugation, and dried at 40°C in air overnight prior to calcination. $Zn_xCo_{3-x}(OH)_6$ was calcined at 400°C in an open air furnace (10 min ramp, 30 min hold) to produce nanoparticulate $Zn_xCo_{3-x}O_4$.

1.3 Spin casting paste preparation

Spin coating pastes were prepared with 10% weight metal oxide, 10% weight hydroxypropyl cellulose (HPC), 40% weight deionized water, and 40% weight ethylene glycol. Homogenization procedures included sonication, vigorous magnetic stirring, and ball milling. Thin film mesoscopic electrodes were prepared using a Laurell WS-650Mz-23NPP spin coater. Spin coated films were subsequently annealed at specified temperatures in various atmospheres. Annealed films were trimmed to an active area of ~0.25 cm^2.

1.4 Analytical methods.

Powder x-ray diffraction (PXRD) studies were performed on a Rigaku Multiflex diffractometer at a scan rate of 2^o 2θ/min on powder samples. Profilometry measurements were performed on a KLA Tencore P-6 profilometer on mesoscopic films with a step edge. Scanning electron microscopy imaging was performed on a FEI Helios NanoLab DualBeam D600 FIB system. TEM imaging was performed on a FEI Titan 80-300 probe aberration corrected scanning transmission electron microscope with a Bruker 4 SDD EDS system for EDS mapping. Bulk elemental composition was measured using an INCA PentaFet −x3 system installed on the FIB system. Optical absorbance measurements were obtained with a Cary 5000 UV-Vis-NIR spectrometer using an integrating sphere. X-ray photoelectron spectroscopy (XPS) and ultraviolet photoelectron spectroscopy (UPS) were performed on a Kratos Axis Ultra DLD X-ray Photoelectron Spectrometer. Mott-Schottky analysis was performed via AC impedance spectroscopy in a three electrode cell with 0.1 M $LiClO_4$ acetonitrile electrolyte. The working

electrode was the $Zn_xCo_{3-x}O_4$ mesoscopic film on FTO, the counter electrode was Pt mesh, and the reference electrode was Ag/AgCl. Electrochemical measurements were performed on a CH Instruments model 604E potentiostat. Seebeck measurements were performed on ~7 μm thick nanoparticle films. The films were contacted to the thermoelectric measurement heating plates with indium metal and measurements were taken after equilibrating for 6 minutes. The Seebeck coefficient was calculated from measurements taken at ~295 K using a Keithley 182 Sensitive Digital voltmeter with the heating plate temperature controlled by a Lakeshore 330 controller.

1.5 Microelectrode Fabrication and Conductivity Measurements.

Microelectrode patterns were fabricated using a literature procedure.[1] Au pads were prepared via electron beam lithography using a Hitachi S4700 SEM on MMA/PMMA films and developed with methyl-isobutyl ketone (MIBK). Chromium and gold were deposited (3 nm and 50 nm respectively) using electron beam evaporation before lift-off with acetone. $Zn_xCo_{3-x}O_4$ films were spin cast on the microelectrode patterns and subsequently annealed. Conductivity measurements were performed using a Keithley 2636A SourceMeter with Signatone micropositioners (S-725) and probe tips (SE-TL).

1.6 Dye-loading measurements.

Dye-loading was quantified using the change in absorbance values (Figure S6) and the maximum extinction coefficient of P1, 5.8 x 10^4 $M^{-1}\cdot cm^{-1}$ at 468 nm.[2]

1.7 DSSC assembly and characterization.

Processed thin films were submerged in a 0.3 mM P1 acetonitrile solution overnight. Platinum counter electrodes were fabricated on FTO glass with a powder-blasted pinhole. A 5 mM H_2PtCl_6 solution in IPA was dropcast on the FTO and annealed at 380 ºC for 30 mins in air to produce the Pt counter electrode thin film. The DSSC was sandwiched using a 25 um thick Surlyn polymer gasket using a custom-built heating apparatus. Sandwiched devices were backfilled with electrolyte (10:1 LiI:I_2 in acetonitrile) using a custom-built vacuum chamber. The cell is sealed with additional Surlyn polymer and a microscope coverslip. The AM 1.5G illumination source was a Newport Oriel 150W Class ABB Solar Simulator which was calibrated before each use with a certified reference Newport 91150 V solar cell. A Keithley 2636A SourceMeter was used for all electrical measurements.

2. Supplemental Figures

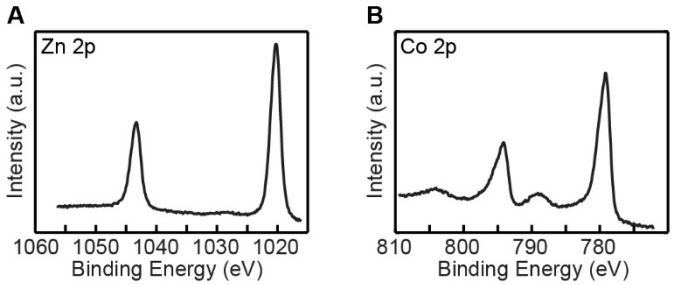

Figure S1. XPS spectra collected in the (A) Zn 2p region and (B) Co 2p region. On the basis of literature data, peaks at 1043.4 eV and 1020.3 eV are assigned to Zn^{2+}.[3] Main peaks at 794.1 eV and 780.0 eV are observed for several cobalt oxidation states. Satellite peaks at 804.1 eV and 789.1 eV are attributed to Co^{3+}.[4]

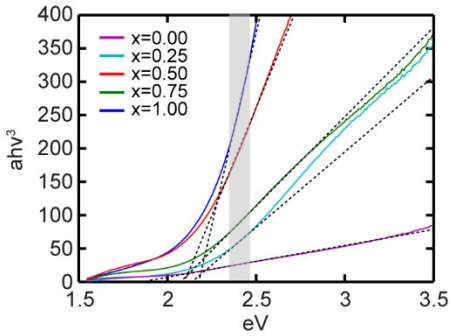

Figure S2. Tauc plot of $Zn_xCo_{3-x}O_4$. Shaded area denotes the region fit to a line. Dashed lines represent the linear fits used to determine the bandgap by intercepts with the horizontal axis.

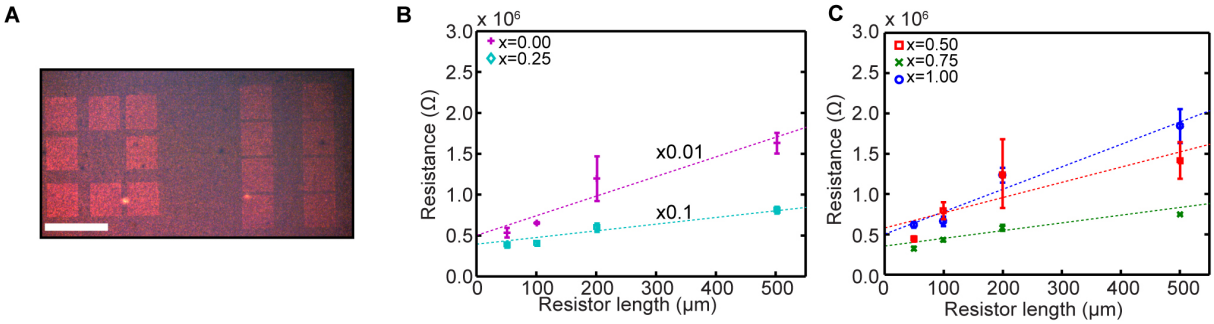

Figure S3. (A) Optical image of a microelectrode pattern consisting of 3 nm Cr and 50 nm Au pads fabricated by electron-beam lithography and metal evaporation. A thin-film 800 nm thick was spin cast on top of the electrodes; scale bar, 1 mm. (B and C) Resistance *vs*. resistor length for $Zn_xCo_{3-x}O_4$, where the resistor length is the distance between microelectrode pads. x = 0.00 data scaled by a factor of 0.01; x = 0.25 data scaled by a factor of 0.1. Dashed lines represent linear fits to data sets for each stoichiometry, and conductivity values were calculated from the slope of the line using a film thickness of 800 nm.

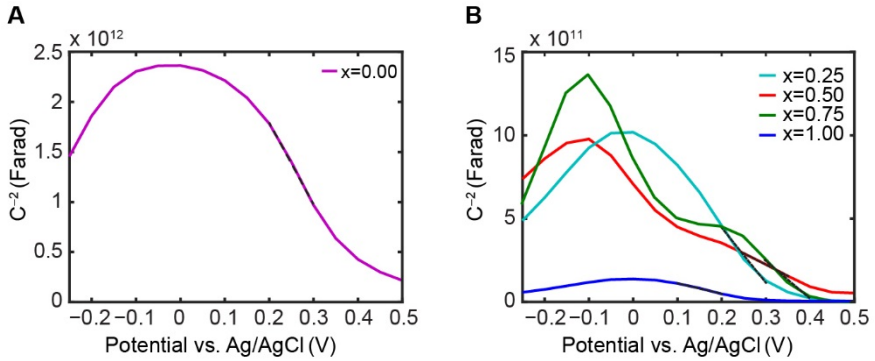

Figure S4. (A-B) Mott-Schottky plots of $Zn_xCo_{3-x}O_4$. Linear fits to extract slopes and valence band edges shown as dashed lines. Mott-Schottky analysis was performed in a three electrode cell at 1 Hz.

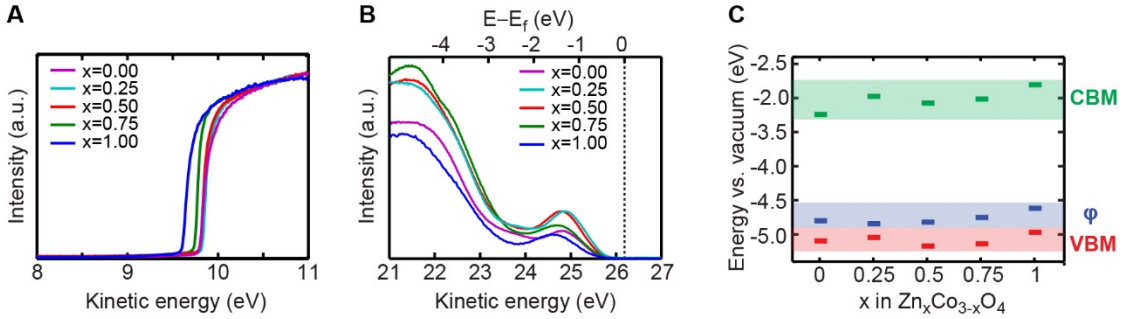

Figure S5. (A) UPS measurement of $Zn_xCo_{3-x}O_4$ in the secondary electron cutoff region. (B) UPS measurement of $Zn_xCo_{3-x}O_4$. Dashed line indicates the Fermi level. (C) Valence band maximum (VBM) extracted from Mott Schottky analysis (red), work function (φ) extracted from UPS measurements (blue), and conduction band minimum (CBM) extrapolated from measured band gaps for all Zn concentrations (green).

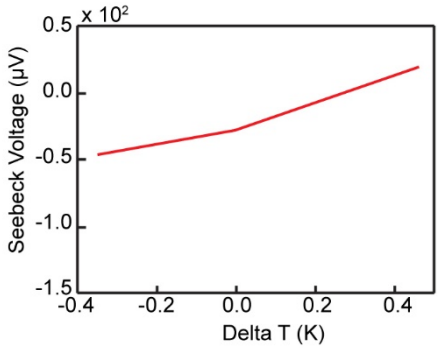

Figure S6. Seebeck measurement for $ZnCo_2O_4$. The Seebeck coefficient measured is 8050 ± 10 $V \cdot K^{-1}$. The Seebeck coefficient is the ratio between the voltage differences over the temperature change.

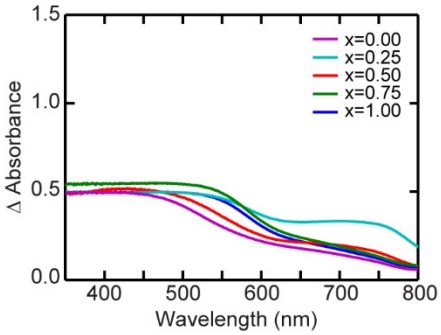

Figure S7. Change in absorbance for $Zn_xCo_{3-x}O_4$ thin films dyed with the P1 molecular chromophore.

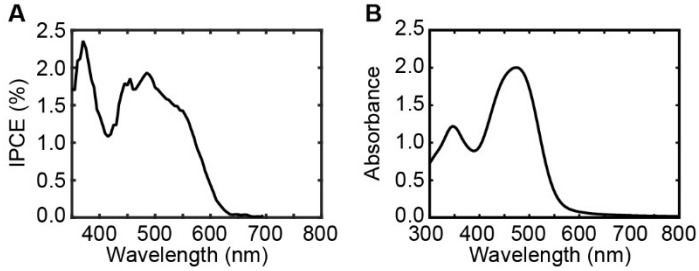

Figure S8. (A) Incident photon-to-current efficiency (IPCE) for a $ZnCo_2O_4$ device sensitized with molecular chromophore P1. (B) Absorbance of P1.

Table S1:

X: $Zn_xCo_{3-x}O_4$	Average J_{sc} (mA·cm^{-2})	Average V_{oc} (mV)	FF (%)	η (%)
0.00	0.11 ± 0.02	106 ± 7	34 ± 2	0.0039 ± 0.0005
0.25	0.17 ± 0.06	111 ± 8	33.6 ± 0.9	0.0064 ± 0.002
0.50	0.21 ± 0.03	108 ± 2	34.3 ± 0.6	0.0080 ± 0.002
0.75	0.27 ± 0.05	114 ± 3	35.2 ± 0.2	0.011 ± 0.002
1.00	0.37 ± 0.09	128 ± 5	33.8 ± 0.1	0.016 ± 0.004

References

1 C. J. Flynn, E. E. Oh, S. M. McCullough, R. W. Call, C. L. Donley, R. Lopez and J. F. Cahoon, *J. Phys. Chem. C*, 2014, **118**, 14177–14184.

2 P. Qin, H. Zhu, T. Edvinsson, G. Boschloo, A. Hagfeldt and L. Sun, *J. Am. Chem. Soc.*, 2008, **130**, 8570–8571.

3 C. A. Dearden, M. Walker, N. Beaumont, I. Hancox, N. K. Unsworth, P. Sullivan, C. F. McConville and T. S. Jones, *Phys. Chem. Chem. Phys.*, 2014, **16**, 18926–32.

4 J. Zhu and Q. Gao, *Microporous Mesoporous Mater.*, 2009, **124**, 144–152.